


## The seismic reflection Moho across the mid-Norwegian continental rifted margin

Gwenn Peron-Pinvidic <sup>1,2</sup> 

The Moho – defined as the boundary that separates the Earth’s crust from the underlying upper mantle at depths of about 5 to 7 km beneath the oceans and 30 to 40 km below continents – has been difficult to pin down with observations. Different methods have yielded a variety of results, suggesting that this simple definition may be misleading. Here, we present high-resolution and deep penetrating seismic reflection data that image the whole margin basement of the mid-Norwegian rift system, including the lower basement, Moho and upper mantle, from the proximal to the outer margin domains. We propose a determination of the seismic reflection Moho in this modern rifted margin context and describe its structural heterogeneity along the margin. Finally, the seismic facies, reflectivity, geometries and structural details of the seismic reflection Moho are described and discussed in terms of tectonic deformation pattern.

<sup>1</sup> NGU Geological Survey of Norway, Leiv Eirikssons vei 39, 7040 Trondheim, Norway. <sup>2</sup> Norwegian University of Science and Technology (NTNU), 7491 Trondheim, Norway. email: [gwenn.peron-pinvidic@ngu.no](mailto:gwenn.peron-pinvidic@ngu.no)

Named after the Croatian seismologist Andrija Mohorovičić who first identified it in 1909 based on seismograms, the Moho was initially defined as a seismic discontinuity—a marked change in propagation velocity of compressional P waves<sup>1</sup>. The velocity of a seismic wave being related to the material density, Mohorovičić interpreted the observed acceleration to be caused by a higher density material present at depth and explained it as corresponding to the crust-mantle boundary (CMB). After decades of research and different observations, Steinhart<sup>2</sup> defined the seismic Moho as the depth at which the P-wave velocity first shows an increase to a value between 7.6 and 8.6 km/s, rapidly or discontinuously. Ideally, this seismological definition is supposed to match the CMB<sup>3</sup> which marks the petrological boundary between the crustal felsic rocks and the underlying ultramafic mantle.

The Moho has been the focus of several major research projects<sup>4–7</sup>, including ambitious drilling campaigns, such as the 1960s US project Mohole<sup>8</sup> specifically designed to drill through the thin oceanic crust of the Mexican Guadalupe Island, or the 1970s soviet Kola Superdeep borehole<sup>9</sup>, on the Russia Kola Peninsula, aimed at sampling the continental Moho. Although unsuccessful, this latter campaign drilled down to 12 km and brought exceptional constraints on velocity discontinuities and seismic reflection patterns within the continental crust. Onshore direct observations of the Moho are possible at some locations, which deeply improved our understanding of the composite nature of the boundary. An oceanic paleo-Moho can be observed for instance in Norway, on the Leka island, with an outcrop juxtaposing lower crustal cumulate peridotites and mantle harzburgites, interpreted as a petrological Moho<sup>10</sup>. Direct onshore access to the continental Moho is scarcer. Observations are possible in the Alps, in the western Val Malenco region (northern Italy) for instance, where a complex petrological transition from the subcontinental upper mantle into the lower continental crust, including gabbroic intrusions, can be studied directly<sup>11</sup>.

For rifted margin studies, the imaging of the Moho is an important constraint in every interpretation protocol. The identification of the base of the continental crust is a very instructive characteristic for evaluating the overall rifting evolution. It allows assessment of the amount of basement thinning and study of the uplift-subsidence evolution of the sedimentary basins. Various research projects investigated the seismic reflection Moho related to extensional settings, such as the marine surveys BIRPS<sup>12</sup> and MONA LISA<sup>13</sup> that provided spectacular images of the Moho in the central North Sea. Major research efforts such as EUROPROBE<sup>14</sup> and LITHOPROBE<sup>15</sup> also provided key information on the depth of the Moho below huge portions of the continents. However, the imaging of the Moho appears non-unique and dependent on the method used for the investigation. The concept of the Moho as a sharp boundary is misleading in its simplicity<sup>16</sup>, for two main reasons: first, as observed in some onshore outcrops, the Moho probably often corresponds to a complex interface rather than to a sharp boundary<sup>17</sup>; and, second, as summarized by Carbonell et al.<sup>7</sup>, the signature of the Moho is to a large degree dependent on the methodology that has been used to obtain the image. Each geophysical method—seismic reflection, seismic refraction, passive seismology, potential fields—being sensitive to specific physical parameters, covering the petrologic, lithologic, seismological, and geophysical characteristics of the boundary. For instance, the seismic reflection Moho may be sensitive to the lithology (e.g., layered lower crust vs. more homogeneous upper mantle) or to the presence of tectonic structures (e.g., shear zones, faults), while the gravity Moho is sensitive to the repartition of the rocks based on their relative densities. As demonstrated by some studies on the mid-Norwegian rifted margin<sup>18</sup>, both geophysical methods may

mismatch considerably in some settings. So, the imaging and interpretation must be handled with care, good information, and, if possible, a combination of high-quality geophysical and geological information. Where available, seismic refraction profiles are considered the most accurate method to locate the Moho, as originally seismically defined.

For this contribution, the focus is set on the seismic reflection Moho. Within the context of the modern mid-Norwegian rifted margin, based on a new seismic reflection dataset<sup>19</sup>, the facies, geometrical variations, and reflectivity pattern of the Moho are described and discussed in conjunction with the margin domains. It is shown below that each structural domain displays specific Moho characteristics.

### Geological context

The data used for this study were located on the Norwegian Continental Shelf. The dataset covers the Møre and Vøring segments of the Mid-Norwegian rifted margin (Fig. 1). This margin experienced a long-lived geological evolution including an orogeny in Silurian times, an orogenic collapse in Devonian times, and a rifting period extending over more than 250 Myr from the Mid-Carboniferous/Permian to the Eocene/Paleocene<sup>20</sup>. The extensional period is very long. It included distinct phases of active tectonic deformation alternating with periods of apparent tectonic quiescence<sup>21</sup>. The resulting conjugate rifted margins are characterized by the juxtaposition of the typical margin domains (proximal, necking, distal) with structural variations in the dip and strike directions<sup>21,22</sup>. Figure 1 displays a map of these domains together with an interpreted seismic reflection profile selected as representative of the general architecture of the margin. The seafloor, top basement, and Moho horizons are displayed to illustrate the mapping strategy carried out in this study<sup>19</sup>.

Typically, the proximal domain shows a continental crust that is slightly thinner, with an overlying relatively thinner sedimentary interval<sup>23</sup>, although important crustal thinning can occur locally<sup>24</sup>. The necking domain corresponds to the domain where the basement is thinned, where typically the Moho and top acoustic basement converge forming a neck geometry<sup>25</sup>. The distal domain is divided into two sub-domains (Fig. 1): (1) continentward, the hyperextension subdomain is usually characterized by series of tilted blocks diminishing in size oceanward<sup>26</sup> and (2) oceanward, the exhumation subdomain corresponds to the areas where the basement (mid-lower continental crust and/or mantle) can be tectonically exhumed<sup>27</sup>. However, it is often difficult to identify and define a top basement and a Moho in these regions, so the exhumation subdomain remains largely unconstrained. The outer domain is mapped as the domain where the tilt and back rotation of the stratigraphic layers witness the presence of faulted blocks at depth in the form of structural ridges<sup>28,29</sup>. It is further characterized by an increased amount of magmatic material identified in the form of sills, dikes, lava flows, and SDRs (seaward dipping reflectors)<sup>30</sup>.

### Mapping strategy

In this study, the Moho is defined as the base of the lower continental crust in the proximal settings, the base of the basement (whatever composition) in the more distal settings, the top of the basement where mantle exhumation is assumed, and the base of the oceanic crust in the oceanic domain. Concretely, for the seismic reflection mapping strategy, the Moho is defined as the envelope bounding at depth a well-identified lower basement reflective body. This body presents a clear seismic facies signal with a series of medium to high amplitude reflectors that form a consistent unit at lower basement depths—usually between 10 and 12 s-twtt in the proximal domain and between 7 and 10

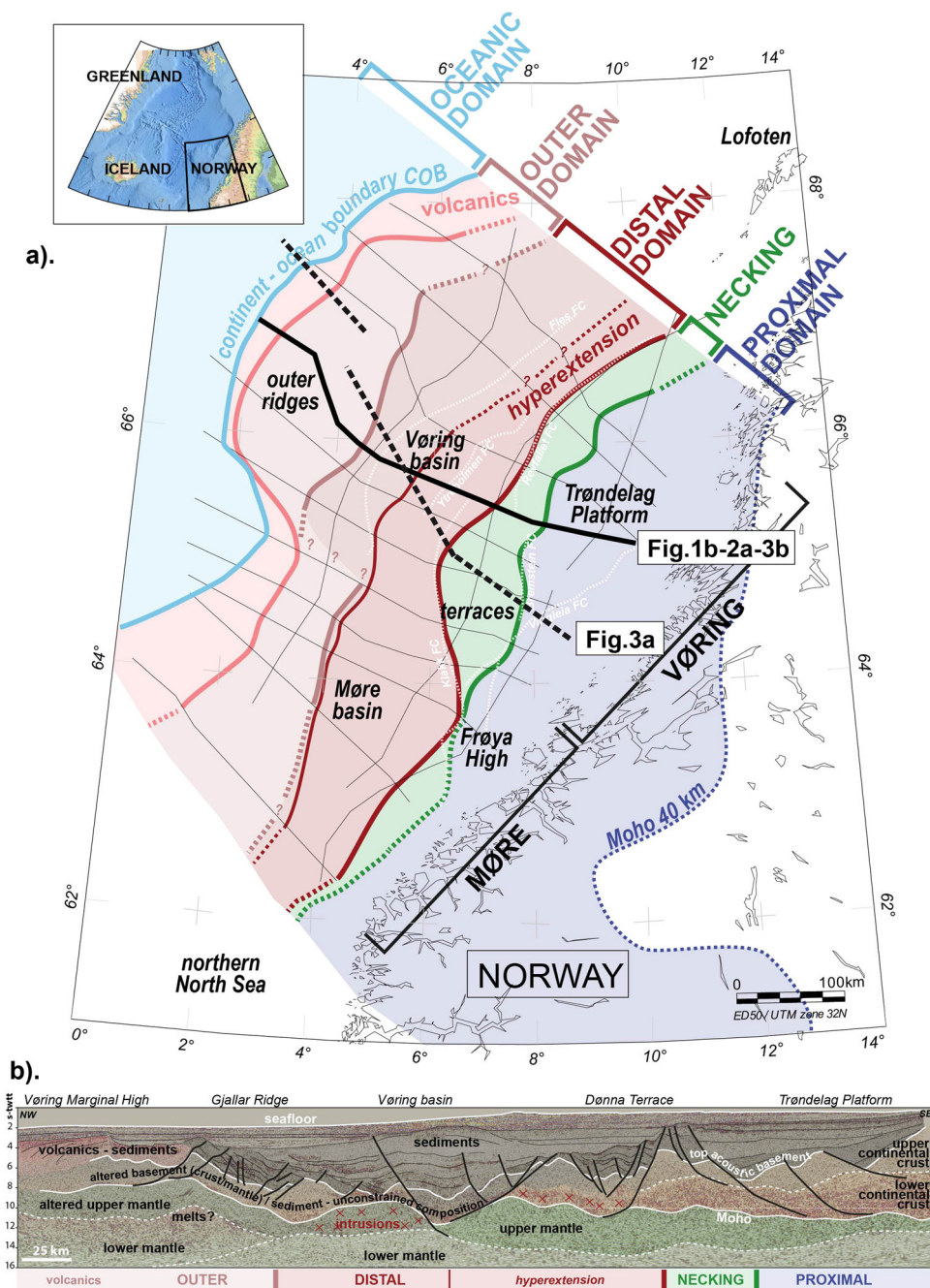


**Fig. 1** Map of the structural domains of the mid-Norwegian continental rifted margin. **a** Map of the study area: the mid-Norwegian rifted margin offshore Norway with the Møre and Vøring margin segments. See top left inset for North-East Atlantic location. The thin black lines show the profiles of the seismic reflection Geox MCG RD119 dataset<sup>53</sup>. The colored polygons represent the different margin domains (proximal, necking, distal, outer, oceanic—see top right bracketed labels). The thick black line localizes the profile presented at the bottom of the figure (panel **b**) and in Figs. 2 and 3. **b** Seismic reflection profile selected as representative of the global architecture of the Norwegian Continental Shelf. The main envelopes (seafloor, top basement, Moho) are drawn as white lines. Dashed white lines represent other important observed seismic facies changes at mid-crustal and mantle depths. The main faults are mapped, together with the main sedimentary and basement units. See the Geological context section for explanations. Modified after Peron-Pinvidic et al. (2022).

s-twt in the more distal settings (Figs. 1 and 2). This definition fits previous interpretations of the Moho in the adjacent North Sea where deep penetrating seismic profiles allowed similar robust identification of the Moho in proximal settings<sup>31,32</sup>. The Moho envelope is confidently defined in the proximal, necking, hyperextended and outer domains where it corresponds to a series of high amplitude discontinuous reflectors - either as a diffuse group of reflectors or as individual reflectors. The signal is

more smeared in the outward part of the distal domain (outer Møre and Vøring basins) where basement exhumation is assumed. As illustrated by similar other long-offset seismic reflection profiles<sup>33,34</sup>, in such settings mapping priority is given to coherency and continuity. The dataset available for this study included 15 profiles with regional coverage. All have been studied and included in the mapping procedure. Where uncertainties appeared, the mapping has been cross-checked and calibrated for

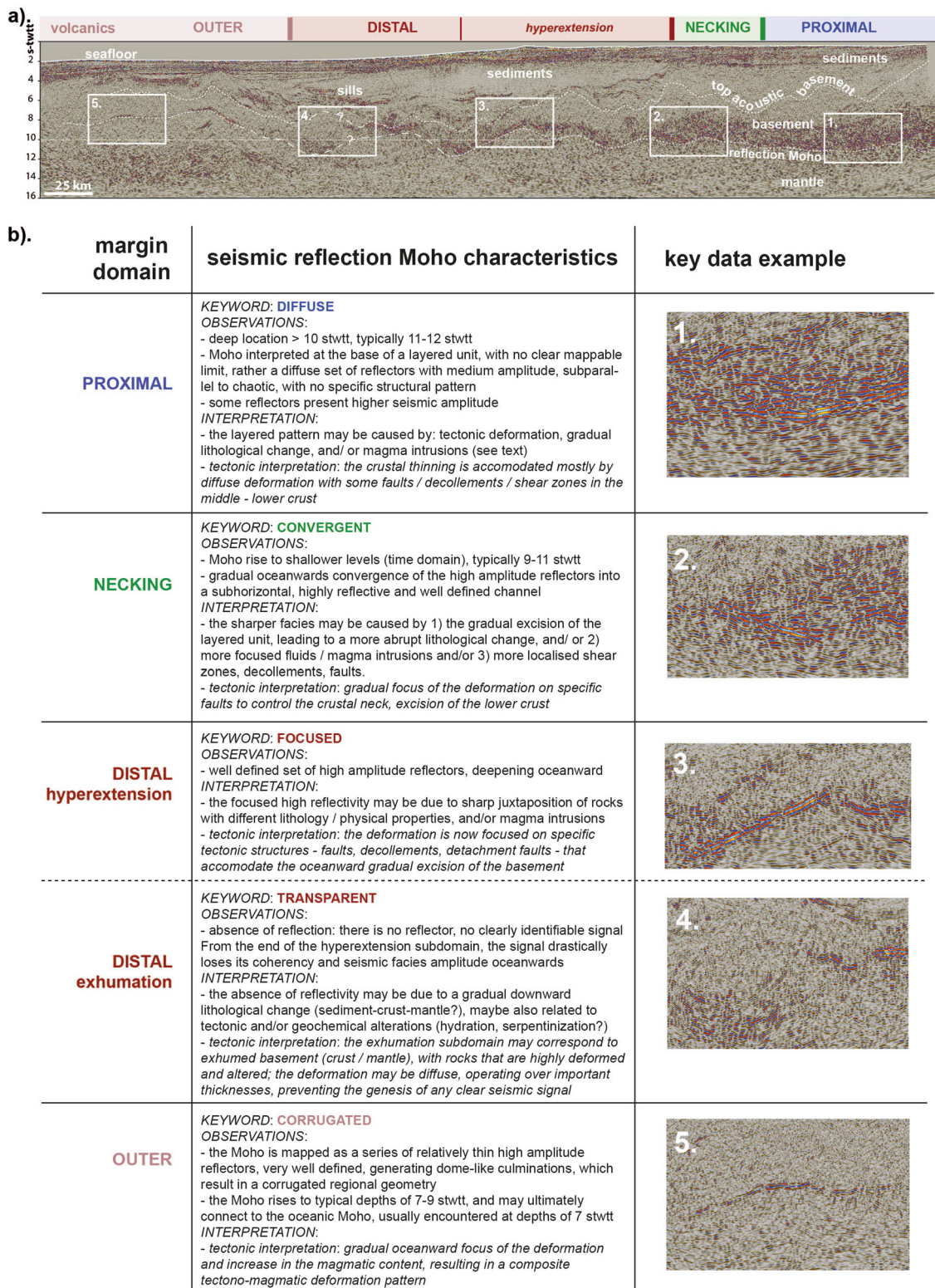


**Fig. 2 List of the seismic facies and geometrical characteristics of the seismic reflection Moho. a** Seismic reflection profile selected as representative of the global architecture of the Norwegian Continental Shelf. See Fig. 1 for location. Geox MCG RDI19 dataset. The top acoustic basement and Moho are outlined with thin dashed white lines. The white boxes locate the profile extracts displayed in the table below. **b** List of the characteristics of the seismic reflection Moho observed in the different rifted margin domains—including a succinct summary of the seismic facies and geometries, and a tentative geologic and tectonic interpretation.

regional coherency together with previous mapping exercises based on other profiles from the dense seismic dataset available in the mid-Norwegian area<sup>27,29,35</sup>. This means that the observations listed here are robust and coherent at the margin scale. However, it should be kept in mind that seismic reflection interpretation is non-unique and interpreter-dependent, as in every geophysical interpretation and modeling exercise. So, alternative mapping of the Moho envelope is possible.

## Results and discussion

**Observations.** The main observation is that the Moho envelope interpreted here presents different characteristics along the margin, from a diffuse reflective pattern, to more focused isolated high amplitude reflectors in the proximal, necking, and hyperextended domains, to the absence of any identifiable reflector in the exhumation subdomain (Fig. 2).

The observation of a layered lower crust vs. a transparent underlying mantle is rather standard, with often a refraction Moho that coincides with the base of the layered body (e.g., the MOIST and DRUM profiles from the BIRPS survey<sup>36</sup>). The layering may be due to various factors<sup>37</sup> and debates remain on the possible nature of the Moho in such contexts. Four main hypotheses can be drawn regarding the nature of the transition from the layered lower crust to the more transparent mantle:

- i. Lithological: a gradual compositional change with ultramafic components becoming dominant as a function of depth could result in a layered pattern depending on the scale of the lithological alternations<sup>3</sup>.
- ii. Metamorphic: the diffuse character of the seismic facies could be associated with long-lasting and distributed metamorphic processes. The Kola borehole has demonstrated that crustal reflectors displaying high reflectivity on seismic reflection profiles can be caused by metamorphic transitions, with possibly rock fracturing due to water saturation<sup>9</sup>.
- iii. Magmatic additions in the form of igneous intrusions<sup>38</sup>: magma crystallized in the lower crust in the form of several pseudo-parallel bodies could cause a well-defined layered pattern. Similarly, lenses of mafic granulites and pyroxenites in an uppermost spinel harzburgite mantle may appear as a layered zone on seismic reflection profiles<sup>3,7</sup>.
- iv. Tectonic: highly strained rocks such as shear zones, potentially up to several kilometers thick, are interpreted as typical in the lower crust and can be imaged as multiple, subparallel seismic reflections<sup>39,40</sup>.

So, the signals observed at lower crust, Moho, and upper mantle depths can be caused by various parameters, including petrologic, magmatic, and tectonic factors. Whatever hypothesis is favored, the Moho corresponds to different physical properties (or variations of) and thus different mechanical properties. These differences imply the existence of a relatively weak interface, probably prone to deformation<sup>41</sup>. Interestingly, this study shows a direct relationship between the seismic reflection characteristics of the Moho and the margin structural domains: the Moho displays distinct seismic facies and reflector geometries in each of the margin structural domains, from a globally diffuse pattern in the proximal domain, to convergent in the necking domain, focused in the hyperextension subdomain, transparent in the exhumation subdomain, and corrugated and discontinuous in the outer domain (Fig. 2). These domains are defined during the different rifting deformation stages and are thus directly related to the tectonic evolution of the margin<sup>21,42</sup>. Based on this, for the discussion that follows, the focus is set on the structural context and relationship to the deformation phases characteristic of each of the margin domains<sup>35,43</sup>.

**Interpretation.** Figure 2 proposes, in the form of a table, seismic extracts illustrating the Moho reflectivity and the seismic facies of the overlying lower crust and the underlying upper mantle observed in the dataset.

1. In the proximal margin, typically between 11 and 12 s-twtt, the Moho shows diffuse seismic facies, separating a layered lower crust and a rather transparent uppermost mantle with no abrupt geometrical change or first-order boundary reflector. Although the background signal is rather chaotic, no clear or systematic cross-cut pattern is observed, so the magmatic intrusion hypothesis (above point iii) is not favored at the margin scale (although local igneous intrusions are probable<sup>38</sup>). The tectonic interpretation proposed here argues that the diffuseness of the seismic facies points in the lowermost crust to a distributed deformation pattern. The crustal thinning that operated in the proximal margin is accommodated by multiple families of faults and shear zones<sup>44</sup>. The ductile layers tend to distribute the deformation on several levels<sup>39</sup>. The observed local high amplitude reflectors showing sharper geometries may correspond to some isolated faults, detachment faults or décollements.
2. In the necking domain, the Moho is mapped at the base of a unit of medium to high amplitude reflectors, organized in a globally oceanward convergent neck pattern. The sharper seismic facies is interpreted to be due to the focus of deformation onto specific tectonic structures, with the gradual excision of the lower crust layered unit, leading to a more abrupt lithological change. Magma intrusions are still probable and can locally participate in the genesis of the seismic reflectivity.
3. In the hyperextension subdomain, the Moho is mapped as the very well-defined set of high amplitude reflectors bounding at depth the series of tilted blocks of the hyperextension margin domain. The focused high reflectivity may be due to a sharp juxtaposition of rocks with different lithology/physical properties, and/or magma intrusions. The tectonic interpretation suggests that the deformation in this margin subdomain is concentrated on specific tectonic structures at lower crustal levels—such as faults, décollements, and detachment faults—that accommodate the oceanward final excision of the continental crust.
4. In the exhumation subdomain, Moho reflections are not observed: both the typical lower crust and Moho signals steadily observed in the more proximal settings are not visible. No clearly identifiable discontinuity is observed. The exhumation subdomain corresponds to an area of the deep margin where the basement is exhumed (mid/lower crust and/or mantle), generating new basement surfaces<sup>45</sup>. The absence of top basement and Moho reflections may be due to a gradual downward lithological/compositional change (e.g., sediments to crust to mantle), including some probable tectonic and/or geochemical/metamorphic alterations related to the intense deformation (e.g., faulting, brecciation, shearing, hydration, metamorphism, serpentinization). Magmatic intrusions cannot be excluded either: although igneous additions in the form of sills and dikes are intuitively associated with bright seismic contrast, the cooling of a local magma chamber may result in “reflection-free bodies”<sup>6</sup>, unidentifiable based solely on seismic reflection investigations.
5. In the outer domain, the Moho is mapped as a series of well-defined discontinuous, relatively thin, high amplitude reflectors (Fig. 2). These form dome-like culminations that result in a corrugated regional geometry. The reflectors are

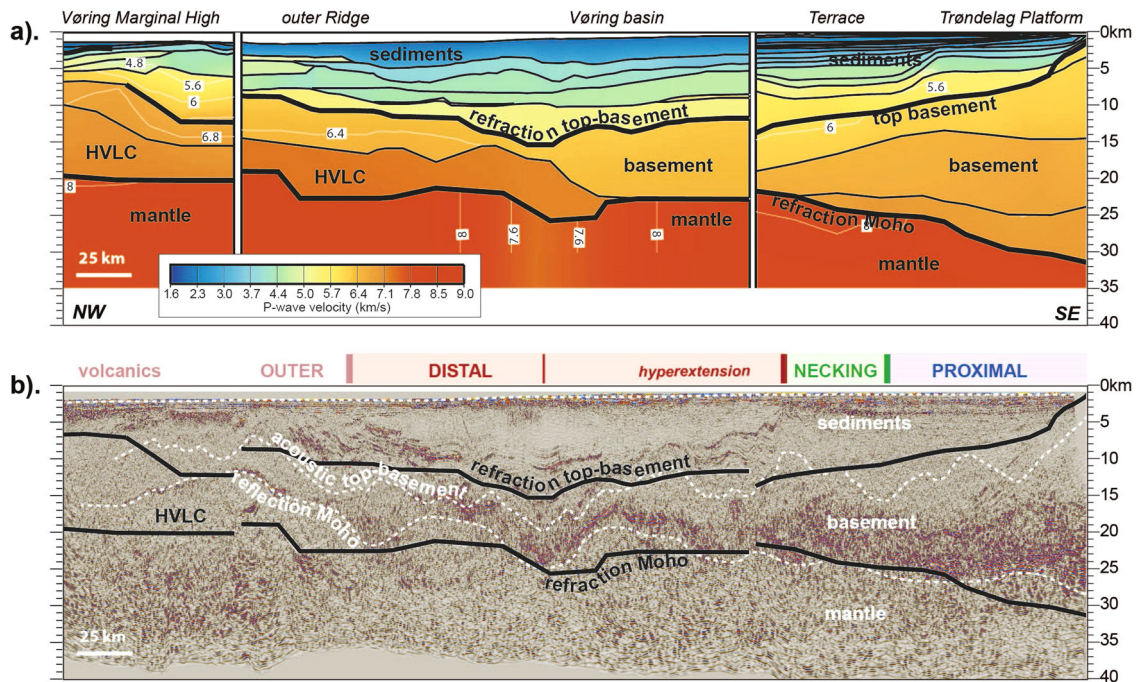


**Fig. 3 Comparison between seismic refraction and seismic reflection Mohos.** **a** Composite seismic refraction profiles remodeled and compiled by Funck et al.<sup>48,49</sup>. The original models are issued from: right-hand segment: the OBS2003 Line 3 from Breivik et al.<sup>50</sup>, middle segment: the Vøring96 Line 10 from Raum et al.<sup>52</sup>, left-hand segment: the OBS2003 Line 11 from Breivik et al.<sup>51</sup>. **b** Depth converted seismic reflection profile selected as representative of the global architecture of the Norwegian Continental Shelf. Same as in Figs. 1b and 2a. See Fig. 1 for location. The top acoustic basement and seismic reflection Moho are outlined with thin dashed white lines. The refraction top basement and Moho modeled based on wide-angle data are displayed with thick black continuous lines. HVLC high-velocity lower crust.

observed at typical depths of 7–9 s-twt and may ultimately connect to the oceanic Moho. The focused high reflectivity pattern is interpreted as an oceanward concentration of the tectonic deformation onto specific structures (e.g., faults, detachment faults, decollements) and an increase in the magmatic content - which agrees with the composite tectono-magmatic deformation pattern characteristic of the outer domain<sup>29,43,46,47</sup>.

**Seismic refraction calibration.** Figure 3 shows a comparison between the seismic reflection Moho interpreted above and the refraction Moho modeled based on wide-angle data. Figure 3a is a composite seismic refraction profile proposed by Funck et al.<sup>48,49</sup>, based on three compiled and remodeled wide-angle models published by Breivik et al.<sup>50,51</sup> and Raum et al.<sup>52</sup>. Figure 3b proposes a depth converted version of the Figs. 1b and 2a seismic reflection profile in time. The depth conversion has been performed based on stacking velocity information. The top basement and Moho envelopes interpreted on the seismic reflection profiles are displayed as white dashed lines, and the top basement and Moho interpreted based on the seismic refraction model are shown as black continuous segments. There appears to be a good match between both datasets in the proximal and necking domains where both the reflection and the refraction Mohos are interpreted at relatively the same levels. This supports the interpretation of the Moho as the top of the upper mantle (P-wave velocity 8 km/s) in these regions. Slight discrepancies appear in the distal margin, which may be due to various factors: first, the reflection and composite refraction profiles are not strictly coincident so some geometrical differences might naturally arise; second, discrepancies may also be related to the different methodological approaches used to model the profiles. However, it is also probable that the mismatch there is related to the complex

deformation history. This area of the rifted margin was subjected to intense tectonic, magmatic, and hydration processes during the hyperextension and exhumation deformation phases, which can lead to severe rock alteration and important changes to the standard geophysical properties<sup>18</sup>. The result is that the refraction Moho defined based on velocity information may differ significantly from the lithological Moho or the structural Moho as mapped on seismic reflection data. Further oceanwards, the difference between the seismic reflection Moho and the seismic refraction Moho is most pronounced in the outer domain. This may point to a need for re-interpretation and/or re-modeling of the reflection and/or refraction data. The presence of a high-velocity lower crust may also influence the mismatch (Fig. 3). However, this body is defined based on velocity (and gravity density) modeling and its composition remains largely unconstrained and debated, preventing robust comparison with the seismic reflection mapping. The outer domain is the margin domain where significant lithological changes are assumed to control the rift to drift processes, including the major magmatic input of the Norwegian-Greenland Sea breakup. Therefore, this domain is a particular area where the mapping and modeling protocols used in the other margin domains may not be directly applicable. Alternative mapping and modeling strategies may need to be developed to encompass the specificities of these frontier regions.

## Conclusions

This contribution focuses on the seismic reflection Moho identification in the mid-Norwegian continental rifted margin. The Geox MCG RDI19 dataset available for the study allows unprecedented observations of the entire basement, including lower crustal rocks, Moho, and upper mantle—from the proximal to the most distal settings of the Norwegian Continental Shelf. The observations support the proposed concept that each margin

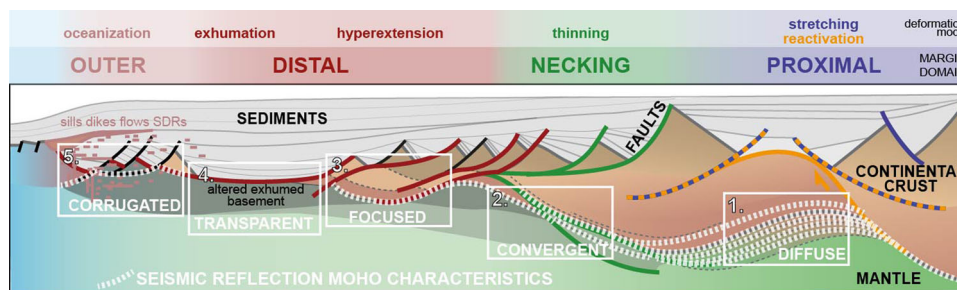


**Fig. 4** The different seismic reflection Mohos identified in the different margin structural domains. Schematic geosection summarizing the main structural characteristics of a standard rifted margin. Modified after Peron-Pinvidic and Osmundsen<sup>54</sup>. The thick dashed white lines illustrate the different seismic reflection Mohos identified in this study, summarizing their main characteristics with keywords: diffuse in the proximal domain, convergent in the necking domain, focused in the hyperextension subdomain, transparent in the exhumation subdomain, and corrugated in the outer domain. The faults are color-coded based on their assumed tectonic evolution related to the deformation phases and margin structural domains.

domain is characterized by a specific seismic reflection Moho type, with particular reflectivity patterns at the transition between the lower crust and the upper mantle (Fig. 4). The Moho seismic reflection facies range from diffuse in the proximal domain, convergent in the necking domain, focused in the hyperextension subdomain, and corrugated and discontinuous in the outer domain. The sharp vs. diffuse seismic facies are discussed in terms of tectonic overprint, and the different reflectivity patterns of the seismic reflection Moho are interpreted to reflect the deformation pattern of each margin domain in the overall rifting evolution. Although this study confirms the Carbonell et al.<sup>7</sup> conclusion on the fact that no universally applicable interpretation of the Moho can be drawn for an entire rifted margin, it is here suggested that each margin structural domain displays specific Moho characteristics. Thus, the identification, mapping, and analysis of the Moho geometries, structural details, and seismic facies may provide good indicators of the basement thinning and rift deformation processes.

## Methods

The imaging of the seismic reflection Moho necessitates deep imaging reflection data. For instance, most of the data available on the Norwegian Continental Shelf are <9–10 s-twt (seconds two-way travel time), which considerably hampers the imaging of the Moho over significant parts of the margin, notably the proximal settings. The Geox MCG Regional Deep Imaging 2019 (RDI19) dataset available for this study is a recent deep towed 16 s-twt long-offset seismic reflection regional dataset<sup>19</sup>. To image the deep rocks, such as the lower crust, Moho, and upper mantle, Geox MCG focused on a long-offset acquisition setting with a large source of 6270 in<sup>3</sup> and a 12-km long streamer with a continuous record of 16 s-twt. The processing was designed to obtain the best imaging of the deep lithological units, including pre-stack noise and diffracted multiple attenuation, pre-migration noise attenuation, migration velocity model analysis, and pre-stack 2D Kirchhoff time migration. With such acquisition and processing parameters, it is an exclusive dataset proposing an unprecedented imaging of the architecture of the Møre and Vøring segments of the Mid-Norwegian rifted margin. The full margin architecture is imaged for the first time including top basement, Moho, and upper mantle within all margin domains, from the most proximal regions in the East to the transition to the oceanic crust in the West (Fig. 1).

## Data availability

The data that support the findings of this study are the property of Geox MCG, and restrictions apply to the availability of these data, which were used under license for the current study, and so are not publicly available. We can, however, provide a version of the seismic profile image presented in Figs. 1–3—without interpretations—on request (please contact the corresponding author). The interpretation and conclusions summarized in this contribution are based solely on the analysis of the final processed profile.

Received: 23 September 2021; Accepted: 23 May 2022;

Published online: 15 June 2022

## References

- Mohorovičić, A. Earthquake of 8 October 1909 (translation). *Geofizika* **9**, 3–55 (1910).
- Steinhart, J. S. Mohorovicic discontinuity. In: *International Dictionary of Geophysics* (ed. Runcorn S. K.) (Pergamon Press, 1967).
- Griffin, W. L. & O'Reilly, S. Y. Is the continental Moho the crust-mantle boundary? *Geology* **15**, 241–244 (1987).
- Prodehl, C. & Mooney, W. D. *Exploring the Earth's Crust—History and Results of Controlled-Source Seismology* (Geological Society of America, 2012).
- Prodehl, C., Kennett, B., Artemieva, I. M. & Thybo, H. 100 years of seismic research on the Moho. *Tectonophysics* **609**, 9–44 (2013).
- Thybo, H. & Artemieva, I. M. Moho and magmatic underplating in continental lithosphere. *Tectonophysics* **609**, 605–619 (2013).
- Carbonell, R., Levander, A. & Kind, R. The Mohorovičić discontinuity beneath the continental crust: an overview of seismic constraints. *Tectonophysics* **609**, 353–376 (2013).
- Horton, E. E. Preliminary drilling phase of mohole project I. Summary of drilling operations. *Aapg Bulletin* **45**, 1789–1792 (1961).
- Ganchin, Y. V. et al. Seismic studies around the Kola Superdeep Borehole, Russia. *Tectonophysics* **288**, 1–16 (1998).
- Furnes, H., Pedersen, R. & Stillman, C. The Leka Ophiolite Complex, central Norwegian Caledonides: field characteristics and geotectonic significance. *J. Geol. Soc.* **145**, 401–412 (1988).
- Müntener, O., Hermann, J. & Trommsdorff, V. Cooling history and exhumation of lower-crustal granulite and upper mantle (Malenco, Eastern Central Alps). *J. Petrol.* **41**, 175–200 (2000).
- Singh, S. C., Hague, P. J. & McCaughy, M. Study of the crystalline crust from a two-ship normal-incidence and wide-angle experiment. *Tectonophysics* **286**, 79–91 (1998).
- MONA-LISA-working-group. MONA LISA—deep seismic investigations of the lithosphere in the southeastern North Sea. *Tectonophysics* **269**, 1–19 (1997).
- Gee, D. G. & Zeyen, H. J. *Lithosphere Dynamics: Origin and Evolution of Continents* (Uppsala, Europrobe Secretariat, 1996).
- Clowes, R. M. Variations in continental crustal structure in Canada from LITHOPROBE seismic reflection and other data. *Tectonophysics* **219**, 1–27 (1993).
- Oliver, J. Changes at the crust–mantle boundary. *Nature* **299**, 398–399 (1982).
- Herzberg, C., Fyfe, W. & Carr, M. Density constraints on the formation of the continental Moho and crust. *Contrib. Mineral. Petrol.* **84**, 1–5 (1983).
- Peron-Pinvidic, G., Osmundsen, P. T. & Ebbing, J. Mismatch of geophysical datasets in distal rifted margins studies. *Terra Nova* **28**, 340–347 (2016).
- Peron-Pinvidic, G., Åkermoen, T. & Leivestad, L. I. The North-East Atlantic Mid-Norwegian rifted margin: Insights from the deep imaging Geox MCG RDI19 dataset. *Tectonophysics* **824**, 229225 (2022).
- Færseth, R. B. Structural geology and basin development of the Norwegian Sea. *Nor. J. Geol.* **100** (2020).
- Faleide, J. I. et al. Structure and evolution of the continental margin off Norway and the Barents Sea. *Episodes* **31**, 82–01 (2008).
- Brekke, H. The tectonic evolution of the Norwegian Sea Continental Margin with emphasis on the Vøring and Møre Basins. In: *Dynamics of the Norwegian Margin: Geological Society Special Publication* (ed Nøttvedt A.) (Geological Society of London, 2000).
- Blystad, P. et al. Structural elements of the Norwegian continental shelf, Part II. The Norwegian Sea Region. *Nor. Petrol. Direct. Bull.* **8**, 0–45 (1995).

24. Peron-Pinvidic, G., Osmundsen, P. T. & Bunkholt, H. The proximal domain of the Mid-Norwegian rifted margin: the Trøndelag Platform revisited. *Tectonophysics* **790**, 228551 (2020).
25. Osmundsen, P. T., Péron-Pinvidic, G., & Bunkholt, H. Rifting of collapsed orogens: successive incision of continental crust in the proximal margin offshore Norway. *Tectonics* **40**, e2020TC006283 (2020).
26. Osmundsen, P. T., Sommaruga, A., Skilbrei, J. R. & Olesen, O. Deep structure of the mid Norway rifted margin. *Nor. J. Geol.* **82**, 205–224 (2002).
27. Osmundsen, P. T. et al. Extension, hyperextension and mantle exhumation offshore Norway: a discussion based on 6 crustal transects. *Nor. J. Geol.* **96**, 343–372 (2016).
28. Ren, S., Faleide, J. I., Eldholm, O., Skogseid, J. & Gradstein, F. Late Cretaceous–Paleocene tectonic development of the NW Vøring Basin. *Mar. Petrol. Geol.* **20**, 177–206 (2003). 130.
29. Peron-Pinvidic, G. & Osmundsen, P. T. Architecture of the distal and outer domains of the mid-Norwegian Vøring rifted margin: insights from the Rån Ridge system. *Mar. Petrol. Geol.* **77**, 280–299 (2016).
30. Artung, U. Regional map of the volcanics of the North-East Atlantic Region. In: *The North-East Atlantic Region: A Reap-praisal of Crustal Structure, Tectono-stratigraphy and Magmatic Evolution* (eds Peron-Pinvidic, G. et al.) (Geological Society of London, 2016).
31. Fossen, H., Gabrielsen, R. H., Faleide, J. I. & Hurich, C. A. Crustal stretching in the Scandinavian Caledonides as revealed by deep seismic data. *Geology* **42**, 791–794 (2014).
32. Gabrielsen, R. H., Fossen, H., Faleide, J. I. & Hurich, C. A. Mega-scale Moho relief and the structure of the lithosphere on the eastern flank of the Viking Graben, offshore southwestern Norway. *Tectonics* **34**, 803–819 (2015).
33. Sauter, D. et al. Evidence for magma entrapment below oceanic crust from deep seismic reflections in the Western Somali Basin. *Geology* **44**, 407–410 (2016).
34. Sapin, F., Ringenbach, J. C. & Clerc, C. Rifted margins classification and forcing parameters. *Sci. Rep.* **11**, 8199 (2021).
35. Peron-Pinvidic, G. & Osmundsen, P. T. The mid Norwegian – NE Greenland conjugate margins: Rifting evolution, margin segmentation, and breakup. *Mar. Petrol. Geol.* **98**, 162–184 (2018).
36. McGeary, S. & Warner, M. R. Seismic profiling the continental lithosphere. *Nature* **317**, 795–797 (1985).
37. Mooney, W. Multigenerative origin of crustal reflectivity: a review of seismic reflection profiling of the continental lower crust and Moho. *Continental Lower Crust* 45–79 (1992).
38. Wrona, T. et al. 3-D seismic images of an extensive igneous sill in the lower crust. *Geology* **47**, 729–733 (2019).
39. Clerc, C., Jolivet, L. & Ringenbach, J.-C. Ductile extensional shear zones in the lower crust of a passive margin. *Earth Planet. Sci. Lett.* **431**, 1–7 (2015).
40. Fazlikhani, H., Fossen, H., Gawthorpe, R. L., Faleide, J. I. & Bell, R. E. Basement structure and its influence on the structural configuration of the northern North Sea rift. *Tectonics* **36**, 1151–1177 (2017).
41. Ranalli, G. & Adams, M. Rheological contrast at the continental Moho: effects of composition, temperature, deformation mechanism, and tectonic regime. *Tectonophysics* **609**, 480–490 (2013).
42. Lavie, L. L. & Manatschal, G. A mechanism to thin the continental lithosphere at magma-poor margins. *Nature* **440**, 324–328 (2006).
43. Peron-Pinvidic, G., Manatschal, G. & Osmundsen, P. T. Structural comparison of archetypal Atlantic rifted margins: a review of observations and concepts. *Mar. Petrol. Geol.* **43**, 21–47 (2013).
44. Naliboff, J. B., Buitter, S. J. H., Péron-Pinvidic, G., Osmundsen, P. T. & Tetreault, J. Complex fault interaction controls continental rifting. *Nat. Commun.* **8**, 1179 (2017).
45. Tugend, J., Manatschal, G., Kuszniir, N. J. & Masini, E. Characterizing and identifying structural domains at rifted continental margins: application to the Bay of Biscay margins and its Western Pyrenean fossil remnants. *Geol. Soc. London Spec. Publ.* **413** (2015).
46. Gillard, M. et al. Birth of an oceanic spreading center at a magma-poor rift system. *Sci. Rep.* **7**, 15072 (2017).
47. Tugend, J. et al. Reappraisal of the magma-rich versus magma-poor rifted margin archetypes. *Geol. Soc. London Spec. Publ.* **476**, SP476.479 (2018).
48. Funck, T. & NAG-TEC-Group. Crustal structure, Chapter 6. In: *Tectonostratigraphic Atlas of the North-East Atlantic Region* (eds Hopper, J. R. et al.) (GEUS, 2014).
49. Funck, T. et al. A review of the NE Atlantic conjugate margins based on seismic refraction data. *Geol. Soc. London Spec. Publ.* (eds Peron-Pinvidic, G. et al.) (2016).
50. Breivik, A. J. et al. Crustal structure beneath the Trøndelag Platform and adjacent areas of the mid-Norwegian margin, as derived from wide-angle seismic and potential field data. *Nor. J. Geol.* **90**, 141–161 (2011).
51. Breivik, A. J., Faleide, J. I. & Mjelde, R. Neogene magmatism northeast of the Aegir and Kolbeinsey ridges, NE Atlantic: spreading ridge-mantle plume interaction? *Geochem. Geophys. Geosyst.* **9** (2008).
52. Raum, T. et al. Crustal structure of the southern part of the Vøring Basin, mid-Norway margin, from wide-angle seismic and gravity data. *Tectonophysics* **355**, 99–126 (2002).
53. Peron-Pinvidic, G. & Åkermoen, T. MCG's Regional Deep Imaging Project: Norwegian Sea 2019. *GeoExpro* **17** (2020).
54. Peron-Pinvidic, G. & Osmundsen, P. T. From orogeny to rifting: insights from the Norwegian 'reactivation phase'. *Sci. Rep.* **10**, 14860 (2020).

### Acknowledgements

Geox MCG is acknowledged for data access and display authorization. Patricia Cadenas, Kim Welford, and an anonymous reviewer are acknowledged for their reviews. Patricia Cadenas and Kim Welford helped improve this manuscript significantly with extremely detailed comments and pertinent and very useful suggestions.

### Author contributions

G.P.-P. performed the study, sketched the figures, and wrote the paper.

### Competing interests

The author declares no competing interests.

### Additional information

**Correspondence** and requests for materials should be addressed to Gwenn Peron-Pinvidic.

**Peer review information** *Communications Earth & Environment* thanks Kim Welford, Patricia Cadenas, and the other, anonymous, reviewer(s) for their contribution to the peer review of this work. Primary handling editors: João Duarte, Joe Aslin, and Clare Davis.

**Reprints and permission information** is available at <http://www.nature.com/reprints>

**Publisher's note** Springer Nature remains neutral with regard to jurisdictional claims in published maps and institutional affiliations.



**Open Access** This article is licensed under a Creative Commons Attribution 4.0 International License, which permits use, sharing, adaptation, distribution and reproduction in any medium or format, as long as you give appropriate credit to the original author(s) and the source, provide a link to the Creative Commons license, and indicate if changes were made. The images or other third party material in this article are included in the article's Creative Commons license, unless indicated otherwise in a credit line to the material. If material is not included in the article's Creative Commons license and your intended use is not permitted by statutory regulation or exceeds the permitted use, you will need to obtain permission directly from the copyright holder. To view a copy of this license, visit <http://creativecommons.org/licenses/by/4.0/>.

© The Author(s) 2022